Available online at www.sciencedirect.com
ScienceDirect
Proceedings of the Combustion Institute 000 (2018) 1–8
Proceedings of the Combustion Institute
www.elsevier.com/locate/proci

Flame–wall interaction effects on the flame root stabilization mechanisms of a doubly-transcritical LO_2/LCH_4 cryogenic flame

C. Laurent [a,*], L. Esclapez [a], D. Maestro [a], G. Staffelbach [a], B. Cuenot [a], L. Selle [b], T. Schmitt [c], F. Duchaine [a], T. Poinsot [b]

[a] *CERFACS, 42 Avenue Gaspard Coriolis, Toulouse Cedex 1 31057, France*
[b] *IMFT, Allée du Professeur Camille Soula, Toulouse 31400, France*
[c] *EM2C, Ecole Centrale Paris, Grande Voie des Vignes, Châtenay-Malabry Cedex 92295, France*

Received 28 November 2017; accepted 25 May 2018
Available online xxx

Abstract

High-fidelity numerical simulations are used to study flame root stabilization mechanisms of cryogenic flames, where both reactants (O_2 and CH_4) are injected in transcritical conditions in the geometry of the laboratory scale test rig Mascotte operated by ONERA (France). Simulations provide a detailed insight into flame root stabilization mechanisms for these diffusion flames: they show that the large wall heat losses at the lips of the coaxial injector are of primary importance, and require to solve for the fully coupled conjugate heat transfer problem. In order to account for flame–wall interaction (FWI) at the injector lip, detailed chemistry effects are also prevalent and a detailed kinetic mechanism for CH_4 oxycombustion at high pressure is derived and validated. This kinetic scheme is used in a real-gas fluid solver, coupled with a solid thermal solver in the splitter plate to calculate the unsteady temperature field in the lip. A simulation with adiabatic boundary conditions, an hypothesis that is often used in real-gas combustion, is also performed for comparison. It is found that adiabatic walls simulations lead to enhanced cryogenic reactants vaporization and mixing, and to a quasi-steady flame, which anchors within the oxidizer stream. On the other hand, FWI simulations produce self-sustained oscillations of both lip temperature and flame root location at similar frequencies: the flame root moves from the CH_4 to the O_2 streams at approximately 450 Hz, affecting the whole flame structure.

Keywords: Cryogenic flame; Flame–wall interaction; Conjugate heat transfer; Real-gas thermodynamics; Flame anchoring

1. Introduction

The global market of space launchers witnessed a marked and fast evolution at the beginning of the 2010s, with increased efforts to drastically cut

* Corresponding author.
E-mail address: laurent@cerfacs.fr (C. Laurent).

https://doi.org/10.1016/j.proci.2018.05.105

down operation costs for example by developing reusable launchers, such as the Falcon 9, designed by SpaceX. These successes were largely due to technological adjustments on liquid rocket engines (LREs), which are now expected to be re-usable, re-ignitable, and able to operate at variable-thrust levels. To meet these constraints, engine designers plan to employ CH_4/O_2 cryogenic combustion, in various thermodynamic states at injection, namely supercritical conditions (LOx/GCH_4) as well as doubly transcritical conditions (LOx/LCH_4). Even though these new LREs are expected to be fully exploitable by 2030, little is known on these new real-gas diffusion flames stabilized on coaxial O_2/CH_4 injectors.

Fundamental reviews of physical processes governing mixing, vaporization, and combustion under transcritical and supercritical conditions are proposed in [1,2]. In the transcritical state (i.e., when pressure exceeds the critical pressure of the fluid, but temperature is below its critical temperature) the fluid thermodynamic properties significantly differ from that of a classic subcritical liquid: as surface tension vanishes jet dynamics are no longer controlled by breakup and atomization, but by mass transfer through turbulent mixing [3,4]. Significant efforts were carried out in the domain of numerical simulation of real-gas combustion with pioneering works [5–7] investigating realistic LO_2/GH_2 shear-coaxial jet flames. It was found that the flame root, dominated by diffusion effects due to large thermophysical properties gradients, is stabilized in a region of high shear behind the injector lip. Meanwhile, experiments of similar supercritical reactive flows have been carried out in different facilities, including the Mascotte test bench operated by ONERA (France) [8]. First the structure of supercritical LO_2/GH_2 shear-coaxial flames was characterized experimentally [9–11], and these results were later recovered numerically with Large Eddy Simulation (LES) [12]. LO_2/CH_4 flames under various injection conditions were also examined experimentally [13] and numerically [14].

Most previous research efforts focused on supercritical flames where oxygen was injected in a dense transcritical state, and fuel (either H_2 or CH_4) as a light supercritical fluid (i.e., at a temperature above its critical temperature). Very few studies tackled the problem of a doubly transcritical regime, where both reactants are injected in a dense transcritical state. The experimental work of Singla et al. [13] is one of the only analysis reporting characteristics of such flames in a realistic shear-coaxial configuration, where the flame displays a specific structure consisting of two concentric conical layers of reactions. As this combustion regime is likely to occur in future LREs, a better understanding of governing phenomena in these specific conditions is highly needed. In addition, most previous numerical approaches relied on two crude simplifications: (1) adiabatic boundary conditions were assumed at the coaxial injector lip [6,7], and (2) simplified chemistry, tabulated [14,15] or based on two-step reduced schemes [12], was employed. However, as briefly mentioned in [6], heat transfer is likely to be important in the coaxial injector lip, due to the combination of very high heat fluxes and thin lips. This effect is expected to be even more pronounced in the case of doubly transcritical combustion, since both reactants are injected in a cryogenic state. As a consequence the resolution of a fully coupled conjugate heat transfer problem is necessary to accurately account for temperatures variations within the wall.

Following these observations, the present work uses a two-dimensional quasi-DNS method with complex chemistry to investigate flame root stabilization mechanisms for a doubly transcritical LO_2/LCH_4 combustion in the Mascotte test rig [13]. This paper addresses FWI effects on flame root stabilization, by considering the unsteady conjugate heat transfer problem, where the flame and the lip temperature field are strongly coupled. To the knowledge of the authors, this is one of the first attempts to simulate doubly transcritical combustion of shear-coaxial flames typical of modern LRE, including FWI and detailed CH_4/O_2 chemistry. Section 2 describes the numerical approach, including details concerning the coupling strategy between the fluid solver and the wall thermal solver, as well as a brief summary of the operating conditions. In Section 3 a detailed kinetic mechanism for CH_4 oxycombustion is derived and validated for high pressure conditions. Finally, Section 4 presents an analysis of flame root structure and dynamics, obtained for a fully coupled simulation and compares them to a case where the lip walls are assumed adiabatic.

2. Numerical approach and operating conditions

The unstructured solver AVBP [14,16] is used to solve the two-dimensional compressible Navier–Stokes equations for a reactive multi-components mixture of fluids. Real-gas non-idealities are accounted for thanks to the Soave–Redlich–Kwong (SRK) equation of state [17]:

$$p = \frac{\rho \bar{r} T}{1 - \rho b_m} - \frac{\rho^2 a_m(T)}{1 + \rho b_m} \tag{1}$$

where $\bar{r}$ is the mixture gas constant, and b_m and $a_m(T)$ are calculated as in [1]. Numerical schemes and boundary conditions are adapted for real gas thermodynamics. A specific local filtering procedure is also used to handle strong density and pressure gradients caused by real-gas non-idealities. More details about this procedure as well as other numerical parameters can be found in [14,18]. Accounting for FWI in the flame root stabilization mechanisms requires solving a fully coupled unsteady conjugate heat transfer problem [19]. Here,

Please cite this article as: C. Laurent et al., Flame–wall interaction effects on the flame root stabilization mechanisms of a doubly-transcritical LO_2/LCH_4 cryogenic flame, Proceedings of the Combustion Institute (2018), https://doi.org/10.1016/j.proci.2018.05.105

Table 1
Injection conditions (mass flow rate, reduced pressures and temperatures), and fluid thermal properties (effusivity e (SI), and effusivity ratio κ_f) for reactants and hot gases (HG). The global equivalence ratio is $\phi_g = 14.3$, the momentum flux ratio is $J = (\rho_F u_F^2)/(\rho_O u_O^2) = 33.3$, and the wall effusivity is $e_w = 1.9 \times 10^4$ (SI).

	Injection conditions			Thermal properties	
	$\dot{m}_{inj}/\dot{m}_{inj}^{O2}$	T_R^{inj}	P_R^{inj}	e_f (SI)	κ_f
O_2	1.0	0.55	1.49	260	75.5
CH_4	3.59	0.62	1.64	2200	8.9
HG		–		80	245

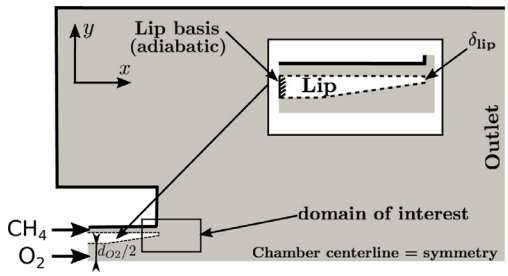

Fig. 1. The two-dimensional computational domain. Thick dark lines represent no-slip adiabatic walls for the fluid domain. Dashed lines are non-adiabatic no-slip walls were fluid and solid domains are coupled. The basis of the lip (hashed line) is an adiabatic boundary condition for the solid domain.

a thermal solver named AVTP is used for the resolution of heat conduction in the coaxial injector lip. Both fluid and thermal solvers are run using a Parallel Coupling Strategy where exchange information is performed through the OpenPalm supervisor [20,21]: the flow solver provides a flux to the conduction solver, while this one provides a temperature to the fluid solver. Between two coupling events, the flow solver (resp. the heat solver) performs α_f (resp. α_w) iterations with a timestep dt_f (resp. dt_w), and exchange frequencies are adjusted such that: $\alpha_f dt_f = \alpha_w dt_w$, in order to ensure physical synchronization and continuity of fluxes and temperatures at the interface.

The Mascotte geometry consists of a coaxial injector with a central oxygen stream of diameter d_{O2} surrounded by an annular methane stream [13,14]. As the present study focuses on flame root stabilization, computations are performed on a two-dimensional domain refined in the near-injector region (Fig. 1). The area of interest, of dimensions $2d_{O2} \times 1d_{O2}$, is located near the injector lip of thickness δ_{lip}, and consists of cells of dimension $0.03\delta_{lip}$ (i.e., a few μm). The diffusion flame reactive thickness (of order 100 μm for the strain rate levels considered here) implies a high resolution of the front with at least 10–16 cells across the reactive thickness. Injection conditions (Table 1) are similar to the operation point T1 in [13]. The only difference is that the chamber pressure has been increased to 75 bar (instead of 54 bar in the experimental study), giving higher reduced pressures. This discrepancy with the experimental conditions of [13] is expected to strongly affect the flow features, and direct comparison with experimental data of [13] is therefore ruled out. However, the aim of the present work is not to quantitatively reproduce experimental results, but rather to qualitatively describe flame stabilization mechanisms occuring in LREs conditions. The computation of this higher pressure operation point was motivated by two elements: (1) a pressure of 75 bar is still relevant to LREs conditions, and it remains a worthy qualitative analysis; (2) at the experimental pressure (54 bar), both reactants pass near their respective critical point as they are heated up, resulting in high fluctuations of pressure and density, due to the numerical resolution of extremely large density gradients combined with highly nonlinear thermodynamics. These numerical oscillations destabilize the computation, unless a significant artificial viscosity is added. On the contrary, at 75 bar these numerical oscillations are less important and do not require the addition of an important artificial viscosity, thus yielding a higher-fidelity computation. One-seventh power-law velocity profiles are imposed at both reactants inlets through NSCBC boundary conditions [22] adapted for real-gas thermodynamics. Only the temperature field in the lip of the central injector is coupled with the fluid domain. The mesh used by the thermal solver is uniform, with a finer cell size of $\delta_{lip}/120$, in order to avoid aliasing due to interpolation errors at the interface. At this point it is interesting to define some quantities relevant to conjugate heat transfer. The fluid effusivity is defined as $e_f = (\rho C_p \lambda)^{1/2}$, with λ the thermal conductivity and C_p the specific heat capacity. We also define the fluid effusivity ratio by $\kappa_f = e_w/e_f$. The effusivity allows to evaluate the ability of a body to exchange heat with its surrounding. Thus for $\kappa_f \gg 1$, temperature at the solid/fluid interface is mostly determined by the wall temperature, and this one can be considered as isothermal. On the contrary, if $\kappa_f \ll 1$ the interface temperature is imposed by the fluid and the wall may be considered as adiabatic. Intermediate values of κ_f correspond to boundaries that are neither adiabatic nor isothermal. Thermal properties (Table 1) show the dominant thermal influence of the cryogenic CH_4 stream

Please cite this article as: C. Laurent et al., Flame–wall interaction effects on the flame root stabilization mechanisms of a doubly-transcritical LO_2/LCH_4 cryogenic flame, Proceedings of the Combustion Institute (2018), https://doi.org/10.1016/j.proci.2018.05.105

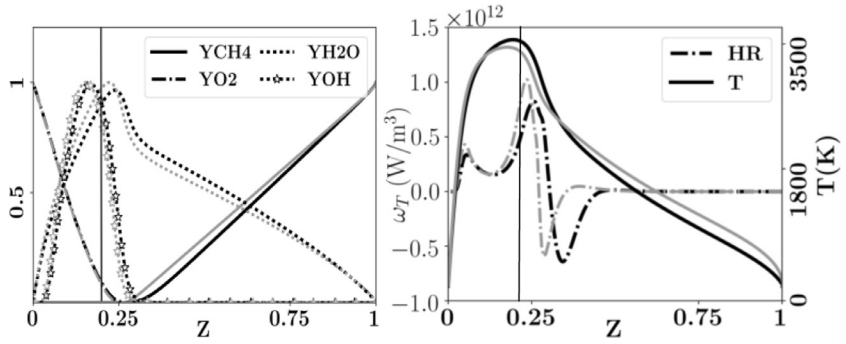

Fig. 2. Comparison between flame structures obtained with GRI3.0 (dark lines), and the reduced GRI_{HP} scheme (light lines), for a CH_4/O_2 counterflow diffusion flame at $P = 75$ bar, $\phi_g = 4$, injection temperatures $T_{inj} = 200$ K, and strain rate $a_T = 1000\ s^{-1}$. Normalized mass fraction profiles of selected species (left), temperature and heat release (right) are presented in mixture fraction space. Vertical lines represent the stoichiometry $Z = 0.20$. Computed with Cantera.

on the lip. None of the interfaces can be considered as adiabatic. Moreover, the wall conduction characteristic time scale is $\tau_w = (\delta_{lip}^2 \rho C_p/\lambda) = 0.6$ ms, which is comparable to that of unsteady motions in the fluid, justifying the need for a conjugate heat transfer problem, where both the solid and the fluid temperatures vary on similar time scales.

3. Methane–oxygen chemistry in LRE conditions

FWI is expected to produce large heat losses at the injector lip, causing strong coupling between heat fluxes and chemistry, and requiring a relatively detailed kinetic scheme to account for low temperature chemistry near the lip. However, fully detailed mechanisms are too computationally expensive for multi-dimensional numerical simulations, and very few reduced mechanisms have been derived and validated for CH_4/O_2 combustion in conditions relevant to those found in LREs. Here a mechanism is derived from the detailed GRI3.0 scheme, through a reduction algorithm proposed by Pepiot-Desjardins and Pitsch [23]. The resulting scheme, denoted as GRI_{HP}, consists of 9 species, 82 reactions, and 7 quasi-steady state species. The reduction process was also applied to other detailed schemes adapted for CH_4 high pressure combustion, such as the RAMEC [24], but the resulting reduced mechanisms did not exhibit any significant difference when compared on diffusion counterflow flames, and the GRI_{HP} was therefore retained for this study. It was validated against data from GRI3.0 on a number of test cases, including 1D-counterflow diffusion flames over a large range of pressures, strain rates, and equivalence ratios (Fig. 2). For all these flames, gaseous O_2 and CH_4 injection is used, because reactants are expected to be fully vaporized when they enter the flame zone [15]. The heat release profiles obtained with both mechanisms are quite similar, presenting three reaction peaks: a primary peak in the rich side of the flame ($Z = 0.25$), a secondary weaker peak in the lean side ($Z = 0.07$), and an endothermic zone in the rich side ($Z = 0.3$). Although the reduced mechanism tends to underestimate the maximum temperature (−2.5%), and to overestimate the primary reaction peak (+20%), an overall satisfactory agreement is observed. A good agreement between GRI3.0 and GRI_{HP} is also found for autoignition delay times in isobaric reactors at high pressure (not shown here). The flame displayed in Fig. 2 is expected to be roughly representative of combustion modes encountered in the numerical simulation, and it is therefore used in the following of this paper as a reference for comparison. In particular, the average volumetric heat release rate $\dot{\Omega}_0 = 3.5 \times 10^{11}$ W/m^3 is used to normalize the heat release computed in the numerical simulations (noted HR^*), and the heat release per flame surface area $\Phi_0 = 40.4$ MW/m^2 (obtained by integration over the flame thickness) is used to normalize the wall heat flux (noted Φ_w^*). The thickness of this flame in physical space is 125 μm, which is much larger than the smallest cell size.

4. Results and discussion

Two simulations were performed, the first one (superscript ^{C}) using conjugate heat transfer at the injector lip (Fig. 1) thanks to the coupling strategy described in Section 2, and the second one (superscript ^{A}) with adiabatic boundary conditions at the lip.

4.1. Flame root structure

Both simulations were run and averaged over 12 ms, which roughly corresponds to 5 convective times relative to a fluid particle in the slow dense oxygen core, or equivalently to 20 characteristic dif-

Please cite this article as: C. Laurent et al., Flame–wall interaction effects on the flame root stabilization mechanisms of a doubly-transcritical LO_2/LCH_4 cryogenic flame, Proceedings of the Combustion Institute (2018), https://doi.org/10.1016/j.proci.2018.05.105

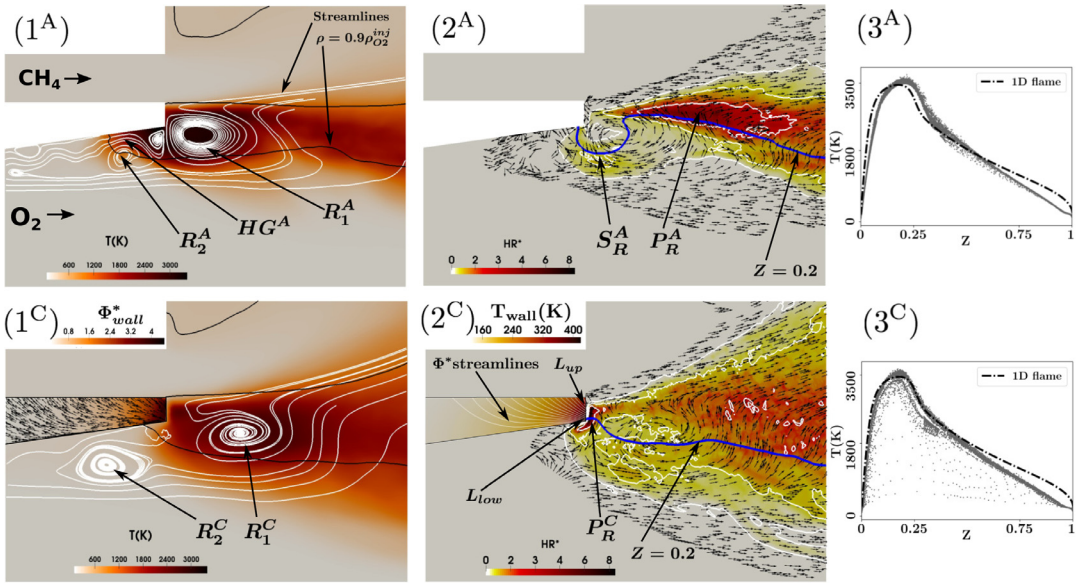

Fig. 3. (1) Averaged temperature field and velocity streamlines in the fluid. Averaged heat flux magnitude and vector field in the wall. (2) Averaged heat release rate and velocity vector field in the fluid. Averaged temperature and heat flux streamlines in the wall. (3) Scatter plot of the flame structure in mixture fraction space, compared to the flame displayed in Fig. 2. Superscripts ^{A} (resp. ^{C}) denote the simulation with adiabatic conditions at the lip (resp. the conjugate heat transfer problem).

fusion times in the solid. Averaged fields of heat release rate, fluid temperature, wall temperature, and heat flux are shown in Fig. 3. The flame root structure obtained in the adiabatic case presents some distinguishable features. In Fig. 3-(1^{A}) Two corotating recirculation zones are visible: a first one (R_1^A) is located in the lip's wake, while the second one (R_2^A) generated by upstream flow separation lies beneath the lip, in the oxygen injection stream. A smaller vortex appears to be trapped and stretched between R_1^A and R_2^A, where a pocket of hot gases (HG^A) is trapped underneath the lip. The density isoline $\rho = 0.9\rho_{O2}^{inj}$ allows to visualize the position of the dense oxygen core, and this one appears to retract under the influence of HG^A, which facilitates cryogenic O_2 pseudo-boiling. In Fig. 3-(2^{A}) , two distinct reaction zones can be identified: an intense primary reaction zone (P_R^A) is located in the lip's wake, at a distance of approximately $1.5\delta_{lip}$ from the lip's end, in a region of high shear between the two streams. This stabilization mechanism is similar to that described in [6] for a LO_2/GH_2 flame. However, unlike the LO_2/GH_2 flame, the present case also displays a weaker secondary reaction zone (S_R^A), situated in the zone of high shear between R_1^A and R_2^A. This secondary reaction zone, anchored onto the lip within the oxygen stream, is fueled through the pocket of hot gases HG^A, which facilitates cryogenic reactants vaporization, and therefore their mixing. This effect is noticeable as S_R^A lies close to the stoichiometry line $Z = 0.2$: gaseous CH_4 invades the dense O_2 stream and is responsible for the anchoring of the secondary flame front beneath the lip. Compared to the LO_2/GH_2 flame studied in [6], this stabilization mechanism is probably due to a significantly higher momentum flux ratio $J = (\rho_F u_F^2)/(\rho_O u_O^2)$ ($J = 33.3$ here, while $J = 0.24$ in [6]). The stabilization mechanism in the adiabatic case seems extremely dependent on the formation and the expansion of the pocket of hot gases HG^A. The temperatures reached by the lip extremity for this adiabatic case range from approximately 300 K to 3500 K, and are not realistic. On the contrary (see Fig. 3-(2^{C})) , the fully coupled problem yields a relatively cold time-averaged lip temperature, which does not exceed 450 K at its extremity. It is also worth noting the large temperature gradient across the lip thickness, varying from 450 K at the lower corner of the lip (L_{low}) to 300 K at the point L_{up} near its upper corner. The cold lip induces significant heat losses at the wall (up to $\Phi^*_w = 4.5$, see Fig. 3-(1^{C})) and prevents the formation of the region of hot gases HG^A seen for the adiabatic case, thereby changing the entire stabilization mechanism. The two main recirculation zones R_1^C and R_2^C still exist, but are slightly more separated than in the adiabatic case, so that no area of high shear is found at their common frontier. Mixing is also notably affected by wall heat losses: because of lower temperatures at the lip, reactants vaporization is less efficient, and gaseous CH_4 is not transported within the oxygen stream,

Please cite this article as: C. Laurent et al., Flame–wall interaction effects on the flame root stabilization mechanisms of a doubly-transcritical LO_2/LCH_4 cryogenic flame, Proceedings of the Combustion Institute (2018), https://doi.org/10.1016/j.proci.2018.05.105

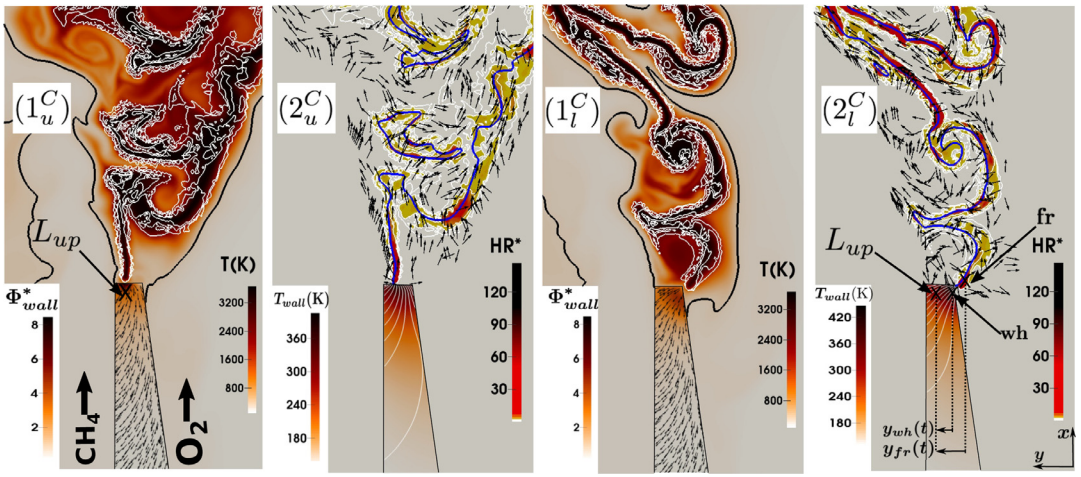

Fig. 4. (1) Instantaneous temperature field and heat release contours in the fluid. The dark line represents the $\rho = 0.9\rho^{inj}_{O2}$ isoline. Instantaneous heat flux magnitude and vector field in the wall. (2) Instantaneous heat release rate and velocity vector field in the fluid. The blue line represents the stoichiometry line $Z = 0.2$. Instantaneous temperature field with heat flux streamlines in the wall. Subscripts $_u$ (resp. $_l$) denote an instant when the flame root is located at the point L_{up} (resp. L_{low}). (For interpretation of the references to color in this figure, the reader is referred to the web version of this article.)

as in the adiabatic case. Only one primary region of reaction (P_R^C) is observed in the coupled simulation. It is located close to the lip extremity, and extends over a long narrow area spreading from the lower corner L_{low} to the point L_{up} closer to the upper corner. This suggests periodic oscillations of the flame, as discussed below. A wider downstream flame brush also tends to indicate large amplitude fluttering of the flame front induced by oscillations of the flame root. Detailed flame structures (Fig. 3-(3^A) and (3^C)) in the mixture fraction space show that with adiabatic boundary conditions, the flame mostly burns in a pure diffusion mode, as its structure is very close to that of the one-dimensional flame presented in Section 3. Conversely, the coupled problem gives a flame that burns in diffusion as well as partially-premixed modes: reactions do not occur close to the wall due to low temperatures, and reactants can mix before reacting.

4.2. Flame root dynamics

In the adiabatic case, the primary reaction zone P_R^A does not exhibit significant oscillations, and similarly to the LO_2/GH_2 flame of [6], it is stabilized in the highly sheared mixing layer between the two reactants streams. The weaker secondary reaction zone S_R^A, anchored beneath the lip is more sensitive to perturbations in the cryogenic oxidizer stream, and undergoes slight intermittentcy. The flame root obtained with FWI effects is more unstable and displays strong periodic self-sustained fluctuations. The primary reaction zone P_R^C oscillates between two positions L_{low} located near the lower lip corner, and L_{up} closer to the upper lip corner. Meanwhile, the lip temperature field changes in phase with the flame root motion: at the lower corner L_{low}, temperature varies between 345 K and 505 K, while it varies between 278 K and 355 K at the upper corner. Snapshots of temperature, heat release, wall heat flux, and wall temperature fields at two instants t_{up} and t_{low}, corresponding to the two distinct flame root locations, are provided in Fig. 4.

When P_R^C is close to the point L_{up}, the flame is subjected to an important shear due to the proximity of the high momentum CH_4 stream. As a consequence, the flame root is a relatively straight and unperturbed segment, followed by large scale vortices downstream. At the same time, wall heat losses contribute to rapidly heat up the upper corner of the lip ($\Phi^*_w = 8.5$), resulting in a relatively homogeneous temperature field across the lip thickness ($T_{Low} = 360$ K and $T_{up} = 340$ K). Conversely, when the main reaction zone P_R^C is located near the lower corner L_{low}, shear is less important due to low velocities in the oxygen stream. The flame root is stretched and rolled up by large scale vortical structures in the mixing layer, and it undergoes a flapping motion. In the meantime, the wall temperature gradient across the lip thickness reaches its maximal value ($T_{Low} = 490$ K and $T_{up} = 280$ K), due to the proximity of the reaction zone to the lip's lower corner. In order to further investigate coupling mechanisms responsible for the self-sustained oscillations affecting simultaneously the flame root and the wall temperature, two quantities of interest are recorded over time. The first one is the radial location $y_{fr}(t)$ of the flame root (noted fr),

Please cite this article as: C. Laurent et al., Flame–wall interaction effects on the flame root stabilization mechanisms of a doubly-transcritical LO_2/LCH_4 cryogenic flame, Proceedings of the Combustion Institute (2018), https://doi.org/10.1016/j.proci.2018.05.105

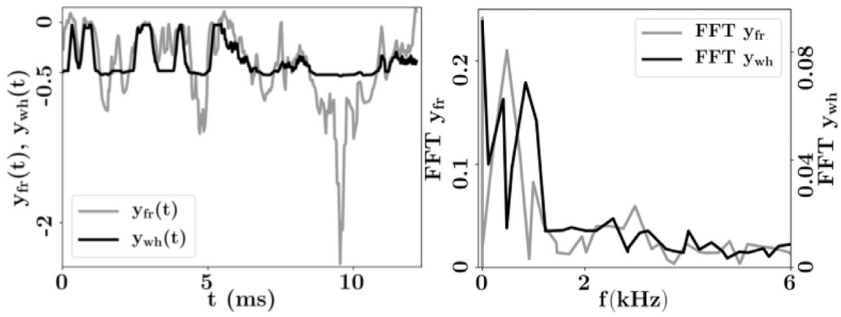

Fig. 5. Left: time-series of the flame root location $y_{fr}(t)$ and the wall hotspot location $y_{wh}(t)$. Right: Fourier spectra associated to these two signals.

and the second one is the radial location $y_{wh}(t)$ of the wall hotspot (noted wh), defined as the point of maximum temperature in the lip (Fig. 4 right). Both locations are normalized by the lip thickness δ_{lip}. Coordinates origin is taken at the point L_{up} indicated in Fig. 4. Temporal evolution and Fourier spectra of the two signals are shown in Fig. 5. A strong correlation between flame root and wall hotspot fluctuations appears. Both are dominated by two modes, with a first fundamental mode at roughly 450 Hz and its harmonic at approximately 900 Hz. Thus, self-sustained oscillations affecting the flame root seem to result from a complex flame/heat transfer coupling at the wall. Pressure fluctuations were also recorded at several locations in the domain, and as resulting spectra did not exhibit any of the previous frequencies, the influence of acoustics was ruled out as a potential cause of the unsteady flame anchoring. The wall hotspot and flame root coupled dynamics can be further studied by considering the difference $\Delta y(t) = y_{wh}(t) - y_{fr}(t)$ (still normalized by the lip thickness δ_{lip}). One-dimensional Dynamic Mode Decomposition [25] is used to isolate the most energetic components of the signals $y_{fr}(t)$ and $y_{wh}(t)$, corresponding to the peaks in Fig. 5. The resulting phase-portrait in the plane $(\Delta y(t), \dot{\Delta} y(t))$ is displayed in Fig. 6. The origin (0,0) in the phase-plane represents instants where wall hotspot and flame root face each other and move at the same speed. A quick examination of the phase-portrait allows to rule out the existence of any distinct closed limit-cycle, as the trajectory is chaotic and alternates between small orbits around the origin (i.e., fr and wh are close to each other and have similar motion), and larger orbits (i.e., fr and wh are far from each other). Most importantly, 4 cusps located near the origin are clearly visible on the trajectory showing that $y_{fr} \approx y_{wh}$ is an unstable equilibrium position. After reaching a cusp, the trajectory is sent back to a larger orbit. These dynamics are very similar to that of a sphere in a forced double-well oscillator, the central bump representing the unstable equilibrium situation where wall hotspot and flame root face each other. The sphere cannot reach exactly the

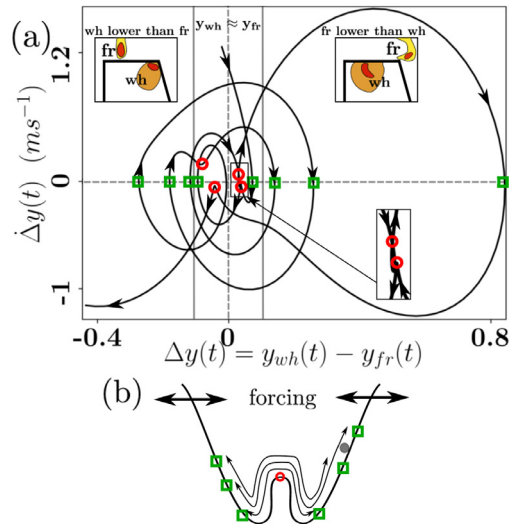

Fig. 6. (a) Phase-portrait of the coupled system in the plane $(\Delta y(t), \dot{\Delta} y(t))$. Red circles indicate unstable equilibrium points at cusps in the trajectory. Green squares represent unstable attracting points. (b) Schematic view of an analogous forced double-well oscillator. (For interpretation of the references to color in this figure legend, the reader is referred to the web version of this article.)

top of the central bump, and slight overshoots in its displacement cause it to fall back on the other side and oscillate on a larger orbit. Analogously, flame root and wall hotspot are never exactly in phase, and overshoots in the flame displacement cause this equilibrium situation to diverge to large values of Δy. Thus, the coupled dynamics consists of a combination of small-amplitude oscillations around the equilibrium state $y_{fr} \approx y_{wh}$, and larger-amplitude oscillations with the flame root position y_{fr} and the wall hotspot position y_{wh} decorrelated from each other. Physically, this unsteady coupling can be explained by unsteady heat convection phenomena occurring in the fluid. (1) When the flame is stabilized near the point L_{up} large vortices downstream of the straight flame root bring hot gases

Please cite this article as: C. Laurent et al., Flame–wall interaction effects on the flame root stabilization mechanisms of a doubly-transcritical LO_2/LCH_4 cryogenic flame, Proceedings of the Combustion Institute (2018), https://doi.org/10.1016/j.proci.2018.05.105

close to the lower corner L_{low} (see in Fig. 4). The lip hotspot then moves from the point L_{up} to L_{low}, and the flame root follows its motion. (2) Conversely, when the flame is stabilized near L_{low}, vortices convect hot gases towards the upper corner, and the reverse mechanism takes place.

5. Conclusions

Two-dimensional high-fidelity simulations have been used to characterize flame root stabilization mechanisms in the case of doubly transcritical LO_2/LCH_4 combustion produced at the lips of a coaxial injector. Flame Wall Interaction (FWI) effects are accounted for by solving the coupled conjugate heat transfer problem at the injector lip, and by using an appropriate detailed kinetic scheme for CH_4 oxycombustion in LRE conditions. Significantly different stabilization mechanisms are found between simulations using adiabatic walls and the fully coupled computations. More precisely, in the former case, the flame is mainly stabilized in a sheared mixing layer between reactants streams, similarly to LO_2/GH_2 flames. However, adiabatic walls appear to facilitate cryogenic reactants vaporization and therefore their mixing. This effect results in the formation of a secondary reaction front within the O_2 injection stream. Conversely, the coupled problem exhibits no stable mixing layer and strong self-sustained oscillations of the flame root and of the temperature field in the lip. Both were found to be bimodal and to oscillate at similar frequencies, indicating a strong influence of heat transfer in the lip on the flame root location. As a result, successive flame root locations were observed (1) in the proximity of the CH_4 stream, where the flame is stabilized by high shear, (2) and in the proximity of the O_2 stream where the flame root is stretched and rolled-up by vortical structures. The chaotic coupled dynamics of this system can be compared to that of a sphere sliding in a forced double-well oscillator. These self-sustained oscillations are expected to be important for the flame response to external forcing, but also for the overall flame stabilization process. Finally, note that this study assumes perfectly smooth injector walls. Although this point was not investigated, flow features taking place at such small scale are expected to be highly sensitive to wall roughness, which could potentially alters the reported flame root stabilization mechanisms.

Acknowledgments

The authors thank Ariane Group, as well as CNES, for their support.

Supplementary material

Supplementary material associated with this article can be found, in the online version, at doi:10.1016/j.proci.2018.05.105.

References

[1] V. Yang, *Proc. Combust. Inst.* 28 (1) (2000) 925–942.
[2] J. Bellan, *Prog. Energy Combust. Sci.* 26 (4) (2000) 329–366.
[3] B. Chehroudi, D. Talley, E. Coy, *Phys. Fluids* 14 (2) (2002) 850–861.
[4] W. Mayer, J. Telaar, R. Branam, G. Schneider, J. Hussong, *Heat Mass Transf.* 39 (8–9) (2003) 709–719.
[5] J.C. Oefelein, V. Yang, *J. Propuls. Power* 14 (5) (1998) 843–857.
[6] J.C. Oefelein, *Proc. Combust. Inst.* 30 (2) (2005) 2929–2937.
[7] J.C. Oefelein, *Combust. Sci. Technol.* 178 (1–3) (2006) 229–252.
[8] L. Vingert, M. Habiballah, P. Vuillermoz, S. Zurbach, 51st International Astronautical Congress, Rio de Janeiro, Brazil (2000).
[9] S. Candel, P. Herding, P. Scouflaire, et al., *J. Propuls. Power* 14 (5) (1998) 826–834.
[10] M. Juniper, A. Tripathi, P. Scouflaire, J.C. Rolon, S. Candel, *Proc. Combust. Inst.* 28 (1) (2000) 1103–1109.
[11] M. Juniper, S. Candel, *J. Propuls. Power* 19 (3) (2003) 332–341.
[12] T. Schmitt, L. Selle, B. Cuenot, T. Poinsot, *C. R. Méc.* 337 (6–7) (2009) 528–538.
[13] G. Singla, P. Scouflaire, C. Rolon, S. Candel, *Proc. Combust. Inst.* 30 II (2) (2005) 2921–2928.
[14] T. Schmitt, Y. Méry, M. Boileau, S. Candel, *Proc. Combust. Inst.* 33 (1) (2011) 1383–1390.
[15] G. Lacaze, J.C. Oefelein, *Combust. Flame* 159 (6) (2012) 2087–2103.
[16] V. Moureau, G. Lartigue, Y. Sommerer, C. Angelberger, O. Colin, T. Poinsot, *J. Comput. Phys.* 202 (2) (2005) 710–736.
[17] G. Soave, *Chem. Eng. Sci.* 27 (6) (1972) 1197–1203.
[18] T. Schmitt, L. Selle, A. Ruiz, B. Cuenot, *AIAA J.* 48 (9) (2010) 2133–2144.
[19] F. Duchaine, S. Mendez, F. Nicoud, A. Corpron, V. Moureau, T. Poinsot, *C. R. Méc.* 337 (6–7) (2009) 550–561.
[20] R. Mari, B. Cuenot, J.P. Rocchi, L. Selle, F. Duchaine, *Combust. Flame* 168 (2016) 409–419.
[21] F. Duchaine, S. Jauré, D. Poitou, et al., *Comput. Sci. Discov.* 8 (1) (2015) 015003.
[22] T.J. Poinsot, S. Lele, *J. Comput. Phys.* 101 (1) (1992) 104–129.
[23] P. Pepiot-Desjardins, H. Pitsch, *Combust. Flame* 154 (1) (2008) 67–81.
[24] E.L. Petersen, D.M. Kalitan, S. Simmons, G. Bourque, H.J. Curran, J.M. Simmie, *Proc. Combust. Inst.* 31 (1) (2007) 447–454.
[25] P.J. Schmid, *J. Fluid Mech.* 656 (2010) 5–28.

Please cite this article as: C. Laurent et al., Flame–wall interaction effects on the flame root stabilization mechanisms of a doubly-transcritical LO_2/LCH_4 cryogenic flame, Proceedings of the Combustion Institute (2018), https://doi.org/10.1016/j.proci.2018.05.105